JOURNAL OF VIROLOGY, Aug. 2005, p. 9862–9871 Vol. 79, No. 15
0022-538X/05/$08.00+0 doi:10.1128/JVI.79.15.9862–9871.2005

Murine Coronavirus Requires Lipid Rafts for Virus Entry and Cell-Cell Fusion but Not for Virus Release

Keum S. Choi,[1] Hideki Aizaki,[1] and Michael M. C. Lai[1,2]*

Department of Molecular Microbiology and Immunology, University of Southern California, Keck School of Medicine, Los Angeles, California 90033-1054,[1] and Academia Sinica, Taipei, Taiwan[2]

Received 30 September 2004/Accepted 13 April 2005

Thorp and Gallagher first reported that depletion of cholesterol inhibited virus entry and cell-cell fusion of mouse hepatitis virus (MHV), suggesting the importance of lipid rafts in MHV replication (E. B. Thorp and T. M. Gallagher, J. Virol. 78:2682–2692, 2004). However, the MHV receptor is not present in lipid rafts, and anchoring of the MHV receptor to lipid rafts did not enhance MHV infection; thus, the mechanism of lipid rafts involvement is not clear. In this study, we defined the mechanism and extent of lipid raft involvement in MHV replication. We showed that cholesterol depletion by methyl β-cyclodextrin or filipin did not affect virus binding but reduced virus entry. Furthermore, MHV spike protein bound to nonraftraft membrane at 4°C but shifted to lipid rafts at 37°C, indicating a redistribution of membrane following virus binding. Thus, the lipid raft involvement in MHV entry occurs at a step following virus binding. We also found that the viral spike protein in the plasma membrane of the infected cells was associated with lipid rafts, whereas that in the Golgi membrane, where MHV matures, was not. Moreover, the buoyant density of the virion was not changed when MHV was produced from the cholesterol-depleted cells, suggesting that MHV does not incorporate lipid rafts into the virion. These results indicate that MHV release does not involve lipid rafts. However, MHV spike protein has an inherent ability to associate with lipid rafts. Correspondingly, cell-cell fusion induced by MHV was retarded by cholesterol depletion, consistent with the association of the spike protein with lipid rafts in the plasma membrane. These findings suggest that MHV entry requires specific interactions between the spike protein and lipid rafts, probably during the virus internalization step.

The fluid-mosaic model proposed by Singer and Nicholson (35) has long been used to explain the organization of membrane. Lipid rafts are defined as the functional lipid microdomains, which consist of cholesterol, sphingolipid, and their associated proteins (32). Although their existence is still debatable, the presence of specific microdomains in biological membranes is a largely accepted concept. Based on studies of model membranes, it is evident that cholesterol and sphingolipid in the membrane can form a highly ordered microdomain, distinct from the disordered liquid-phase membranes of surrounding phospholipids (21). This organization confers resistance to cold-detergent treatment and flotation to light buoyant density (7). Both properties are commonly used to identify lipid rafts. Recent studies have suggested that lipid rafts play a role in a wide range of cellular events, including signal transduction, apoptosis, cell adhesion, migration, synaptic transmission, organization of the cytoskeleton, and protein sorting during endocytosis and exocytosis (7, 15, 34, 38). In addition to their roles in the cells, lipid rafts function as a docking site for the entry of viruses, bacteria, and toxins, as well as virus assembly and budding (19, 29, 36).

Both enveloped and nonenveloped viruses use lipid rafts in various ways to enter the cells (10). In the case of nonenveloped viruses, virus entry begins with the attachment of virus to receptors, followed by internalization of virus by invagination of the plasma membrane and intracytoplasmic vesiculation. Lipid rafts are involved in the direct association of some viruses with their receptors and internalization of virus through caveolae. Simian virus 40 is internalized into caveolae (26) after its binding to the receptor, major histocompatibility complex 1, which normally is not detected in lipid rafts (9). Echovirus type 1 is also internalized into caveolae through the interaction with its receptor, α2β2-integrin, which is in the lipid raft (22). The entry of enveloped viruses involves the attachment of virus to the receptor, followed by fusion between virus and cell membrane, which can be either plasma or endosomal membrane. Therefore, lipid rafts may be involved in the viral entry process in several different ways, including the association of viral glycoproteins with lipid rafts of either the viral envelope or the target membrane or the association of cellular receptors with lipid rafts. Hemagglutinin of influenza virus (31), gp120-gp40 of human immunodeficiency virus type 1 (HIV-1) (27), and glycoprotein of Ebola virus (3) are associated with lipid rafts in the virion. The E1 protein of Semliki Forest virus is inserted selectively to the cholesterol-rich microdomains of the target membrane (1). CD4 and CCR5, the receptor and the coreceptor, respectively, of HIV-1 are associated with lipid rafts (12, 20, 28).

Involvement of lipid rafts in virus assembly and budding in influenza virus, Ebola virus, and HIV-1 has also been well studied. Hemagglutinin and neuraminidase of influenza virus cluster in lipid rafts and recruit M1 matrix protein to lipid rafts to promote virus assembly (2). The matrix protein VP40 of Ebola virus, which is important in virus assembly and budding, localizes and oligomerizes in lipid rafts (25). Moreover, Pr55^{gag}

* Corresponding author. Mailing address: Department of Molecular Microbiology and Immunology, University of Southern California, Keck School of Medicine, 2011 Zonal Ave., HMR 401, Los Angeles, CA 90033-1054. Phone: (323) 442-1748. Fax: (323) 442-1721. E-mail: michlai@usc.edu.

of HIV-1, like gp120/gp40 (27), also associates with lipid rafts during virus assembly (17, 24).

Although there was no direct evidence that lipid rafts are involved in coronavirus replication, previous studies have implied that cholesterol and cholesterol-related environments may regulate coronavirus replication; supplementation of cholesterol in the culture medium resulted in marked enhancement of mouse hepatitis virus (MHV)-induced cell fusion (11), and a hypercholesterolemic diet increased the susceptibility of mice to MHV-3 infection (6). In the case of human coronavirus 229E (HCoV-229E), virus entry was inhibited by depletion of cholesterol, resulting in the disruption of viral association with the cellular receptor, CD13 (23). Moreover, knockdown of caveolin-1 affected the entry of HCoV-229E but not its binding (23), although the significance of caveolin-1 in virus entry has yet to be demonstrated. On the other hand, Thorp and Gallagher showed that cholesterol-rich microdomains were crucial for the entry and fusion of MHV, but the MHV receptor (MHVR) did not associate with lipid rafts; anchoring of the MHV receptor to lipid rafts did not enhance MHV infection (37). These results indicate that cholesterol-rich microdomains are implicated in the viral entry in yet another uncharacterized mechanism.

Here, we report that MHV does not incorporate lipid rafts into the virion and binds to nonraft membrane but shifts to lipid raft membrane for virus entry. The depletion of cholesterol from the target cells does not affect virus binding but interferes with subsequent virus entry. Furthermore, the viral spike (S) protein is not associated with lipid rafts on the Golgi membrane, which is the site of virus assembly and budding (18), but is associated with lipid rafts on the plasma membrane, which is involved in cell-cell fusion. These results explain how lipid rafts are involved in MHV virus entry and cell-cell fusion but not in virus release. We also suggest that MHV entry requires a relocalization of the viral spike protein on cellular membrane during virus entry, probably involving cellular factors associated with lipid rafts.

MATERIALS AND METHODS

Cells, viruses, and antibodies. DBT cells (16), a mouse astrocytoma cell line, were cultured in Eagle's minimal essential medium (MEM) supplemented with 7% newborn calf serum (NCS), 10% tryptose phosphate broth, and streptomycin-penicillin. Human embryonic kidney cell line 293A was cultured in Dulbecco's modified essential medium supplemented with 10% fetal bovine serum. MHV-A59 was amplified in DBT cells and maintained in MEM containing 1% NCS. Modified vaccinia virus Ankara that expresses T7 RNA polymerase was a kind gift from Bernard Moss and amplified in BHK21 cells.

The polyclonal anti-MHV-A59 antibody was produced in rabbits by injection of purified MHV virion. The monoclonal anti-MHVR (CC1) was kindly provided by Kathryn V. Holmes. Monoclonal anti-transferrin receptor, anti-flotillin, and anti-syntaxin 6 were purchased from Zymed Laboratories (San Francisco, CA), BD Biosciences (San Jose, CA), and Stressgen (Victoria, British Columbia, Canada), respectively.

Plasmids. cDNA encoding the viral spike protein was generated by reverse transcription-PCR (RT-PCR) from RNAs extracted from purified MHV virions and then cloned into pcDNA3.1 TOPO (Invitrogen, Carlsbad, CA). Truncated mutants of S protein were made from the cDNA of S protein using specific sets of primers. cDNA that expresses MHV receptor, which is a murine carcinoembryonic antigen gene family member (designated mCGM1), was generated from mouse liver and cloned into a mammalian expression vector, pECE (40).

Cholesterol depletion, replenishment, and detection of uptake of viral RNA. DBT cells were seeded in 12-well plates and at 90% confluency were incubated with either 10 mM methyl-β-cyclodextrin (MβCD; Fluka, Milwaukee, WI) or 2 μg/ml filipin (Sigma, Milwaukee, WI) in MEM at room temperature for 30 min and 1 h, respectively. In the cholesterol replenishment experiments, cells were first incubated with MβCD in MEM for 30 min. The medium was replaced afterward by MEM containing 1 mM cholesterol (Sigma, Milwaukee, WI) for 1 h at room temperature. After the treatment, the medium was replaced by MEM containing 7% NCS, and cells were incubated for up to 24 h. Cholesterol levels in MβCD-treated cells were assayed by using the Amplex Red Cholesterol Assay kit (Molecular Probes, Eugene, OR). Cell viability was assayed by using WST-1 reagent, purchased from Roche (Indianapolis, IN). This assay was based on measurement of the activity of mitochondrial dehydrogenases produced by the viable cells. The enzymatic activity was detected by cleavage of WST-1 to formazan, which was quantified by measuring absorbance at 440 nm. Briefly, cells were seeded in 96-well plates; 10 μl of WST-1 was added to the cells, followed by a 1-h incubation at 37°C. The absorbance was measured with an enzyme-linked immunosorbent assay reader at wavelengths of 420 to 480 nm with a reference wavelength of >600 nm.

To detect viral RNA uptake, untreated or MβCD-treated cells were infected with MHV-A59 at a multiplicity of infection (MOI) of 10. After 1h of virus adsorption, the cells were washed three times with phosphate-buffered saline (PBS) and harvested at 1, 2, 3, and 4 h postinfection (p.i.). Total RNAs were isolated by phenol-chloroform extraction and ethanol precipitation. MHV RNA was detected by RT-PCR using primers specific for the 5′ untranslated region (5′ UTR).

Purification of ^{35}S-labeled virion. DBT cells were infected with MHV-A59 at an MOI of 10; after 1-h virus adsorption, cells were further incubated in MEM containing 1% NCS for 5 h. Cells were rinsed with Met/Cys-free MEM (Sigma, Milwaukee, WI) once and then starved in MEM containing 1% dialyzed NCS for 30 min, followed by addition of 100 μCi of ^{35}S-translabeling mixture (ICN, Irvine, CA). Radiolabeled viruses were harvested at 16 h p.i. and purified by sucrose gradient centrifugation. Briefly, supernatant from the cell culture was clarified by centrifugation at 4,500 × *g* for 30 min at 4°C and then overlaid over 30% to 50% sucrose in NTE (0.5 M NaCl, 10 mM Tris-HCl, 1 mM EDTA, pH 7.4), followed by ultracentrifugation in a Beckman SW28 rotor at 28,000 rpm for 3.5 h. The sucrose interface was collected and pelleted by ultracentrifugation at 100,000 × *g* for 1 h. The purified virions were resuspended in either MEM for the binding experiment or NTE for further purification on continuous sucrose gradients (20% to 60%) in a Beckman SW 41 Ti rotor at 37,000 rpm for 16 h. Samples were collected into 1-ml fractions.

Membrane flotation analysis. Cells were lysed with hypotonic buffer (10 mM Tris-HCl, pH 7.4, 1 mM EDTA) and passed through a 21-gauge syringe 20 times. The lysates were centrifuged at 1,400 × *g* for 5 min at 4°C to remove cell debris and nuclei. The postnuclear supernatant was either untreated or subjected to treatment with 1% TX-100 at 4°C or 37°C for 1 h before ultracentrifugation on a 10%, 55%, and 63% discontinuous sucrose gradient in a Beckman SW41Ti rotor at 37,000 rpm for 16 h at 4°C. Samples were collected into 1-ml fractions and further used for immunoprecipitation or immunoblotting.

In vitro binding assay of virion. Radiolabeled and purified virion (10^6 cpm) was incubated with either untreated DBT cells or 10 mM MβCD-treated DBT cells (10^6), at 4°C or 37°C for 1 h. After being bound, cells were washed with PBS three times and then lysed with hypotonic buffer, followed by treatment with 1% TX-100 at 4°C or 37°C for 1 h. To isolate the detergent-resistant membranes, membrane flotation analysis was done as described above. Each fraction was immunoprecipitated with polyclonal anti-MHV antibody to detect viral proteins.

Separation of plasma and Golgi membranes. Cells (2.5×10^7) were infected with MHV-A59 at an MOI of 10. At 6 h p.i., cells were incubated with 100 μCi of ^{35}S-translabeling mixture (ICN, Irvine, CA). At 10 h p.i., cells were harvested and resuspended in 0.5 ml homogenization buffer (0.25 M sucrose, 1 mM EDTA, 10 mM HEPES-NaOH, pH 7.4), followed by passage 20 times through a 21-gauge syringe. The homogenates were centrifuged at 2,000 × *g* for 10 min. The pellet was resuspended in the homogenization buffer; the centrifugation was repeated, and the two supernatants were combined. The supernatants were centrifuged at 100,000 × *g* for 1 h, and the pellets, which contained membrane fractions, were dissolved in 0.75 ml of 30% (wt/vol) iodixanol (Axis-Shield PoC AS, Oslo, Norway). Membrane fractions were loaded at the bottom of a step-density gradient of iodixanol (2.5, 10, 17.5, and 25%[wt/vol] iodixanol; 2.5 ml per step), prepared from a stock solution diluted in homogenization buffer. The gradients were centrifuged at 37,000 rpm for 3.5 h in a Beckman SW41Ti rotor and fractionated into 0.8-ml fractions; each fraction was used for immunoprecipitation and immunoblotting with specific antibodies. For the subsequent membrane flotation analysis, fractions from either plasma membrane or Golgi membrane were pooled and concentrated to 0.1 ml using centricon YM50 (Millipore, Bedford, MA) with repeated dilutions with hypotonic buffer. Samples were further subjected to membrane flotation analysis as described above.

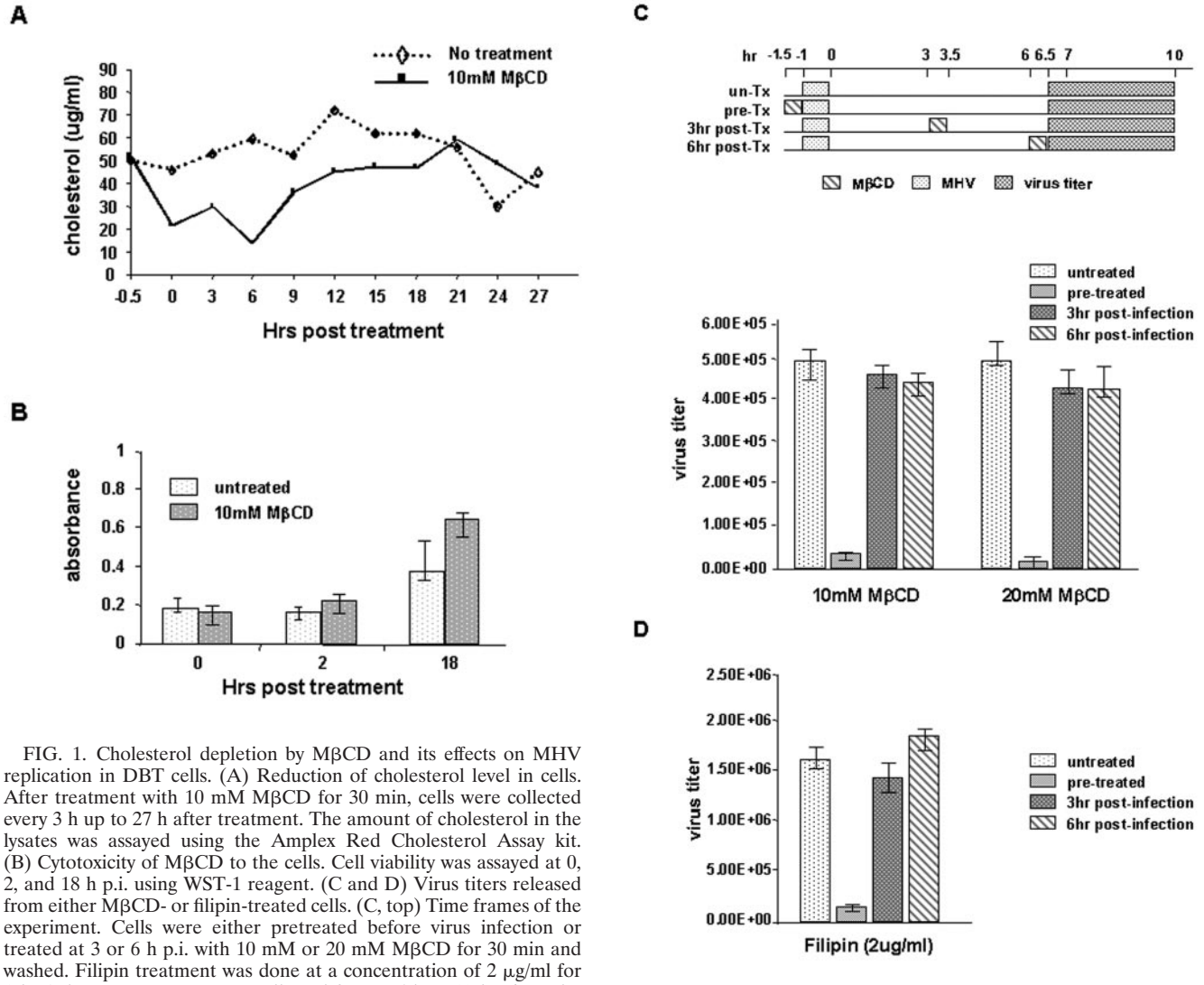

FIG. 1. Cholesterol depletion by MβCD and its effects on MHV replication in DBT cells. (A) Reduction of cholesterol level in cells. After treatment with 10 mM MβCD for 30 min, cells were collected every 3 h up to 27 h after treatment. The amount of cholesterol in the lysates was assayed using the Amplex Red Cholesterol Assay kit. (B) Cytotoxicity of MβCD to the cells. Cell viability was assayed at 0, 2, and 18 h p.i. using WST-1 reagent. (C and D) Virus titers released from either MβCD- or filipin-treated cells. (C, top) Time frames of the experiment. Cells were either pretreated before virus infection or treated at 3 or 6 h p.i. with 10 mM or 20 mM MβCD for 30 min and washed. Filipin treatment was done at a concentration of 2 μg/ml for 1 h. Culture supernatant was collected from 6.5 h to 10 h p.i., and a plaque assay was performed. Samples were duplicated and experiments repeated three times. Arrow bars indicate the standard deviations of three independent experiments.

RESULTS

Virus entry, but not other steps, of viral replication requires lipid rafts in the target membranes. To address the mechanism of involvement of lipid rafts in MHV replication, cholesterol was first depleted from DBT cells by treating the cells with 10 mM MβCD for 30 min at room temperature. The cholesterol level in the cells was reduced by almost 50% immediately after the treatment and remained low for nearly 6 h. It returned to the normal level by 10 to 20 h posttreatment (Fig. 1A). This treatment was not toxic to the cells, as the cell viability was comparable to that of untreated cells (Fig. 1B). To examine the effects of cholesterol depletion on virus replication, cells were treated with 10 mM MβCD for 30 min at various time points postinfection (Fig. 1C, top), namely, untreated, pretreated, at 3 h postinfection, and at 6 h postinfection. Virus titers were determined from the supernatants collected from 6.5 to 10 h p.i. (Fig. 1C). While pretreatment of cells with MβCD completely inhibited virus production, treatments at any time point postinfection did not affect the virus titers, even at a higher concentration of MβCD (20 mM) (Fig. 1C). A similar pattern of inhibition of virus production was also observed when the cells were treated with another cholesterol-depleting drug, filipin (Fig. 1D). This result indicates that cholesterol depletion affected a very early step, most likely virus entry, of virus replication cycle.

To confirm the inhibitory effect of MβCD on virus entry, the viral RNA inside the cells at early time points after virus infection was detected by RT-PCR using the 5′ UTR-specific primers. This RNA represents the viral RNA inside the cells as a result of virus entry. In untreated cells, viral RNA was detected inside the cells beginning at 1 h postinfection. In contrast, after the MβCD treatment, the viral RNA was not detected until 4 h postinfection, when viral RNA replication had begun. Uptake of viral RNA was restored to a level similar to that in the untreated cells after cholesterol was replenished (Fig. 2). This result suggests that virus entry was specifically blocked by cholesterol depletion.

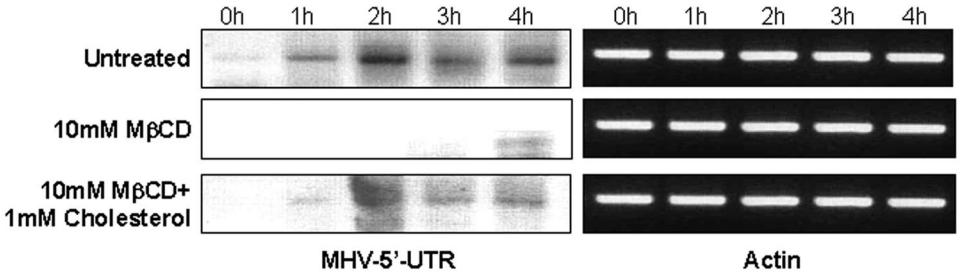

FIG. 2. The effect of MβCD on viral RNA uptake. Cells were either untreated or treated with 10 mM MβCD for 30 min and then infected with MHV-A59. In the cholesterol replenishment experiment, MβCD was removed after the 30-min treatment, and cells were incubated with MEM containing 1 mM cholesterol for 1 h before viral infection. Total cellular RNAs were isolated at 0, 1, 2, 3, and 4 h p.i. MHV RNA was detected by RT-PCR using 5′ UTR-specific primers. RT-PCR of actin mRNA was used as a control.

To understand the mechanism of inhibition of virus entry by cholesterol depletion, we examined whether MβCD affected virus attachment. DBT cells were pretreated with 10 mM MβCD for 30 min and then incubated with radiolabeled MHV for 1 h at 4°C. After the cells were washed with PBS twice to remove the unbound virion, the bound MHV was measured by scintillation counting of cell extracts. The radiolabeled MHV bound to both the untreated and MβCD-treated cells to a similar extent (10 to 12% of the input virus) (Fig. 3A), indicating that virus attachment was not affected by the MβCD treatment. Interestingly, the amount of bound radiolabeled MHV was significantly reduced by the MβCD treatment when the virus-cell binding experiment was performed at 37°C (Fig. 3A). Since incubation of MHV with cells at 37°C induced the entry of virus into cells, this result implies that cholesterol depletion interfered with virus entry at a step subsequent to virus binding. The reduction of the bound virus most likely reflected the dissociation and/or degradation of the virus from the cell surface at 37°C if virus entry did not occur. We also found that MβCD treatment did not affect the surface expression level of MHV receptor (data not shown). These results together suggest that cholesterol is involved in virus entry at a step after virus attachment to the MHV receptor.

To address the mechanism of involvement of cholesterol in virus entry, we next examined the possibility that MHVR naturally associates with lipid rafts or becomes associated with lipid rafts only after virus binding. Lysates from the MHVR-overexpressing 293A cells were treated with 1% TX-100 at 4°C for 1 h, and then membrane flotation analysis was performed. In the absence of the detergent treatment, all of MHVR was detected in membrane fractions; but after treatment with 1% TX-100 at 4°C, most of MHVR was in the detergent-soluble fractions (Fig. 3B). As controls, flotillin, a lipid raft marker, was found in the detergent-resistant membrane, whereas transferrin receptor was found in the detergent-soluble membrane. These results suggested that MHVR was not associated with lipid rafts. We then proceed to study the possibility that MHV infection might induce the relocalization of MHVR to lipid rafts. The results showed that most of MHVR still was detected in the detergent-soluble fractions after virus infection (Fig. 3B). Therefore, very little MHVR shifted to lipid rafts upon virus binding. Our results were consistent with the results from Thorp and Gallagher (37), which also showed that MHVR did not associate with lipid rafts during the virus entry step.

These results raised the puzzling question why MHV entry required cholesterol. We considered the possibility that MHV interacted with lipid rafts in the target membrane directly or indirectly after virus binding to the MHVR. To address this possibility, the radiolabeled virions were incubated with the MHVR-overexpressing 293A cells at 37°C for 1 h, and the lysates were subjected to membrane flotation analysis, followed by immunoprecipitation with polyclonal anti-MHV antibody. The results showed that after virus binding at 4°C, most of the viral S and nucleocapsid (N) proteins were associated with the membrane that was disrupted by treatment with 1% TX-100 at both 4°C and 37°C (Fig. 4A, left), consistent with the previous interpretation that virus binds to MHVR on the nonraft membrane. Interestingly, after virus binding at 37°C, a portion of viral S protein became resistant to treatment with 1% TX-100 at 4°C but remained disruptable by treatment with 1% TX-100 at 37°C (Fig. 4A, right), consistent with the interpretation that it is associated with lipid rafts. A portion of viral S protein was also detected with detergent-soluble fractions, which most likely represent the viral protein released into the cytosol after virus entry. Some of the N protein was also associated with the detergent-soluble membrane after virus binding at 4°C, consistent with the idea that the virus remained attached to the membrane without entering the cells. The status of N protein at 37°C was less clear; it was not detected without the detergent treatment probably because, after virus entered the cells, it was in a structure not amenable to analysis without detergent treatment.

When the same experiment was performed using the MβCD-treated cells, the same result was obtained when the virus binding was carried out at 4°C, namely, viral S and N proteins stayed associated with the nonraft membrane (Fig. 4B, left). This result was consistent with the previous finding that the MβCD treatment did not affect the association of viral proteins with membrane (Fig. 3A). However, most of the viral S and N proteins were lost from the cells after incubation of MHV at 37°C with the MβCD-treated cells (Fig. 4B, right). This result was consistent with the previous binding experiment showing that the amount of bound radiolabeled virus was greatly reduced when virus was incubated at 37°C with the MβCD-treated cells (Fig. 3A). We conclude that virus entry

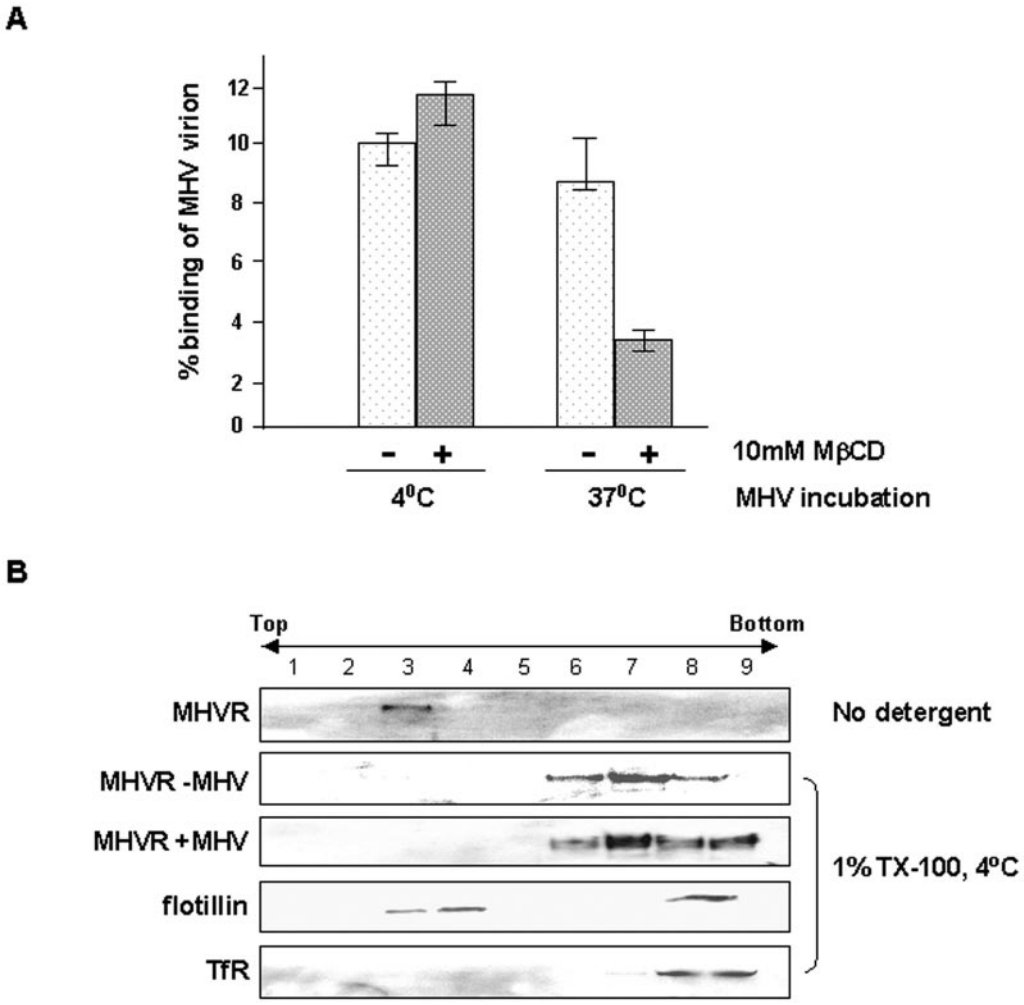

FIG. 3. Effects of cholesterol depletion on virus binding and association of MHV receptor with lipid rafts. (A) Binding of radiolabeled MHV virion. ^{35}S-labeled MHV virion (10^6 cpm) was incubated with either untreated or MβCD-treated cells for 1 h at 4°C or 37°C. Unbound virion was removed by being washed three times with PBS. Cells were harvested and resuspended in hypotonic buffer, and the radioactivity was determined with a scintillation counter. Each sample was done in triplicate, and bars indicate standard deviation. (B) Association of MHVR with lipid rafts. MHVR-overexpressing 293A cells were either uninfected or infected with MHV-A59, and membrane flotation analysis was done after treatment for 1 h with 1% TX-100 at 4°C. MHVR was detected by immunoblotting. Flotillin and transferrin receptor were used as positive and negative control, respectively, for lipid raft association.

induced by incubation at 37°C requires subsequent interaction of MHV proteins with lipid rafts after virus binding.

These results imply that virus entry may involve a redistribution of viral and/or cellular proteins on either viral or cellular membranes at a step subsequent to the virus binding to MHV receptor and that the process involves the shift of viral and/or cellular factors from nonraft membrane to lipid rafts.

Lipid rafts are not incorporated into MHV virion. We next explored the possibility that MHV particles may contain lipid rafts in the envelope. We attempted to alter the cholesterol levels in the virion by treating the cells with MβCD and then examining the properties of virus particles produced from the cholesterol-depleted cells. We first compared the buoyant density of the virus, since the cholesterol composition of the viral envelope has been reported to affect the buoyant density of other viruses, such as human immunodeficiency virus (8). Virus particles released from the MβCD-treated cells had the same buoyant density as that from the untreated cells (Fig. 5A), suggesting that cholesterol is not a significant component of MHV virion.

Next, we performed the membrane flotation analysis of virus particles to examine whether any viral proteins were associated with lipid rafts in the virion. A significant portion of S and N proteins were present in the membrane fractions, but all of them shifted to soluble fractions after treatment with 1% TX-100 at 4°C for 1 h, indicating that viral proteins in the virion were associated with nonraftraft membrane (Fig. 5B).

Next, we examined whether intracellular viral proteins were associated with lipid rafts during virus assembly and budding. MHV is known to assemble and bud on the Golgi membrane (18); however, some S protein is also transported to the plasma membrane, where it mediates cell fusion but is not involved in virus assembly. We separated the Golgi membrane from total cellular membranes by iodixanol gradients (Fig. 6A). Syntaxin

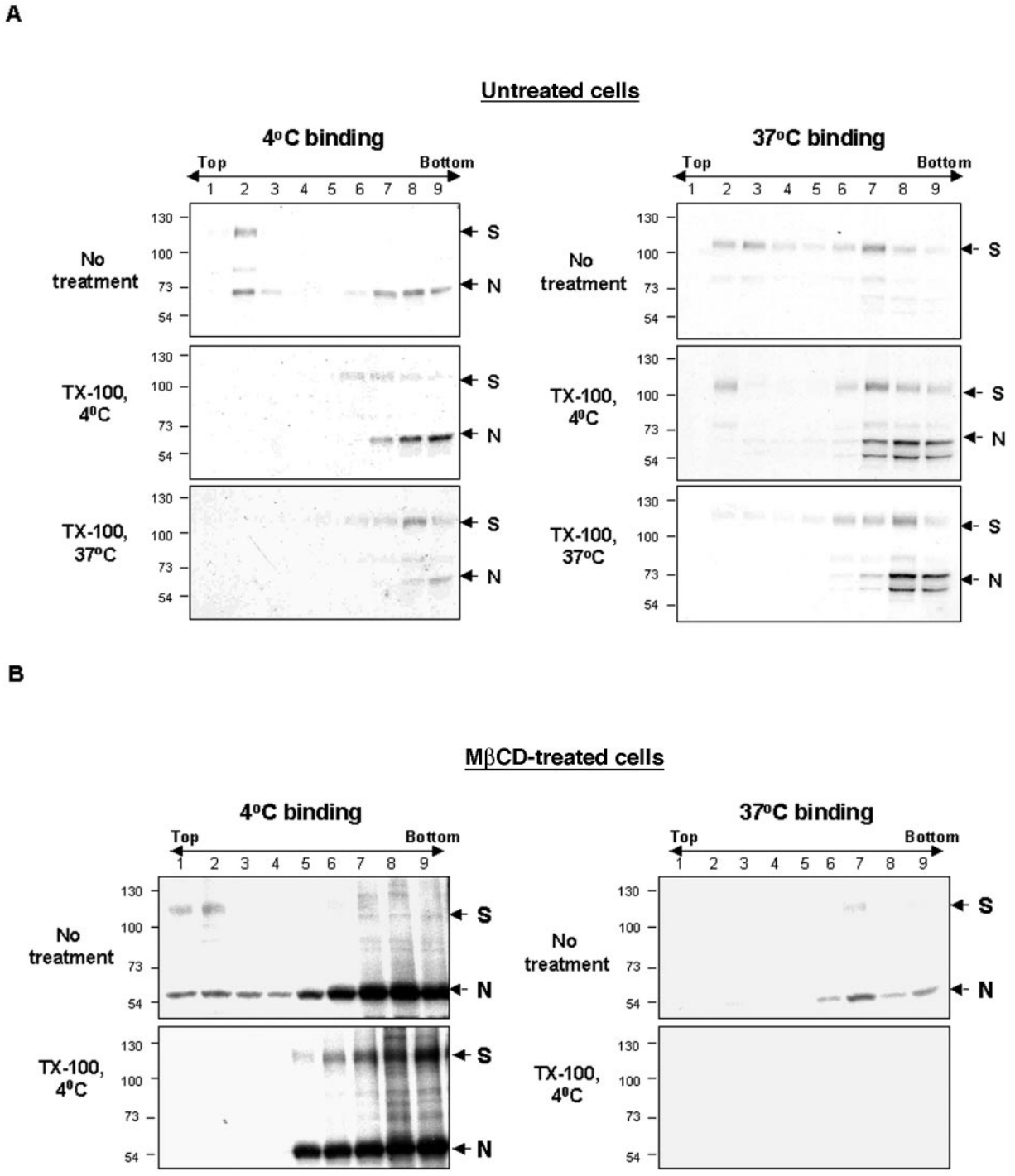

FIG. 4. Redistribution of MHV virion during virus entry. (A) Raft-association of viral proteins during virus entry. ^{35}S-labeled MHV virion (10^6 cpm) was incubated with MHVR-overexpressing 293A cells for 1 h at either 4°C (left) or 37°C (right). Lysates were treated with 1% TX-100 for 1 h at 4°C or 37°C, and membrane flotation analysis was subsequently done. Viral S and N proteins were detected by immunoprecipitation with polyclonal anti-MHV antibody. (B) Effect of cholesterol depletion on the association of viral protein with lipid rafts. MHVR-overexpressing 293A cells were pretreated with 10 mM MβCD for 30 min, and then radiolabeled virus was added and incubated at either 4°C (left) or 37°C (right) for 1 h. Lysates were treated with 1% TX-100 for 1 h at 4°C, followed by membrane flotation analysis. The exposure time for the both panels was the same.

6 (5) and transferrin receptor (14) were used as the markers for Golgi and plasma membranes, respectively. As expected, S proteins were detected in both plasma and Golgi membranes. Fractions representing plasma membrane or Golgi membrane were pooled separately, and detergent resistance of viral proteins was examined by membrane flotation analysis. All of the S and N proteins from Golgi membranes were detected in detergent-soluble fractions, confirming that viral proteins were

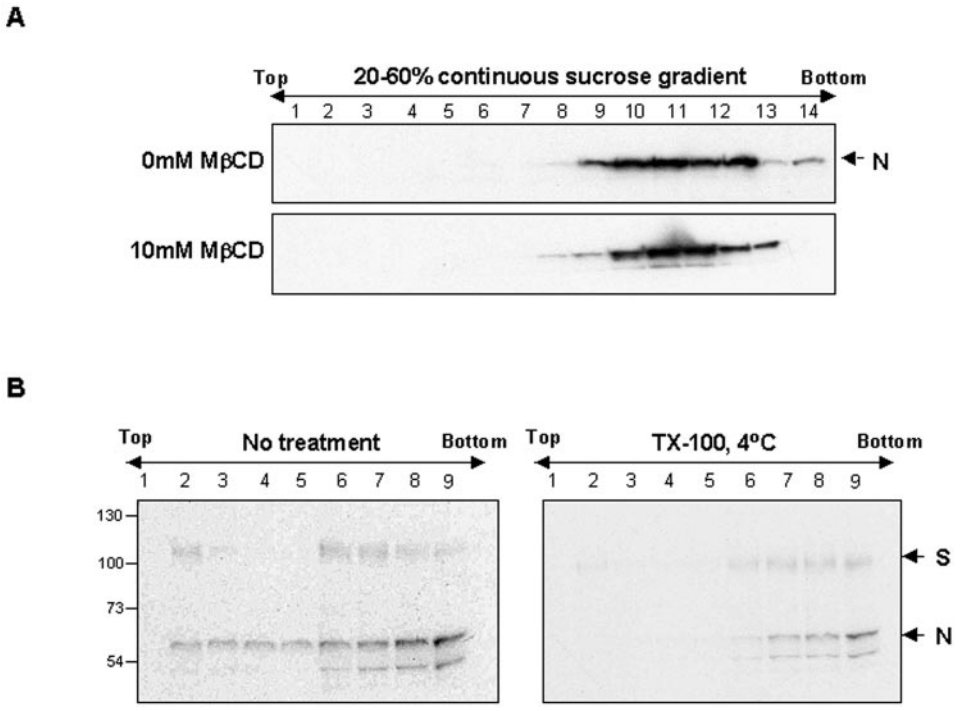

FIG. 5. Lack of incorporation of lipid rafts into MHV virion. (A) Buoyant density of virion produced from cells untreated or treated with 10 mM MβCD. MHV from the culture supernatant was purified by two-step sucrose centrifugation. Samples were collected into 1-ml fractions, and viral N proteins were detected by immunoblotting. (B) Lack of association of viral proteins with lipid rafts in the virion. ^{35}S-labeled MHV virion was treated with 1% TX-100 for 1 h at 4°C, and then membrane flotation analysis was done. The viral S and N proteins were detected by immunoprecipitation with polyclonal anti-MHV antibody.

not associated with lipid rafts during virus assembly and budding (Fig. 6B, right). In contrast, a small fraction of S protein from plasma membrane was resistant to treatment with 1% TX-100 at 4°C (Fig. 6B, left, fractions 2 to 5), indicating its association with lipid rafts.

These results were consistent with the previous experiments (Fig. 1C), which showed that virus titers were not affected by the MβCD treatment if this treatment was performed anytime after virus infection. We conclude that MHV does not incorporate lipid rafts into virion, in contrast to many other enveloped viruses (36).

Cell-cell fusion requires lipid rafts. MHV infection induces morphological changes in cells by inducing cell-cell fusion. Therefore, we asked whether cell-cell fusion was affected by cholesterol depletion. DBT cells were treated with 10 mM MβCD either before virus infection or at various time points after infection (2 or 4 h p.i.). Syncytium formation was examined at 6 and 8 h postinfection (Fig. 7). When cells were pretreated with MβCD, cell-cell fusion was completely blocked, most likely as a result of the inhibition of virus entry. Surprisingly, cell-cell fusion was much delayed when MβCD treatment was done at 2 or 4 h p.i. Under these conditions, the titer of the virus released from the cells was not affected (Fig. 1). This result indicates that cell-cell fusion, in contrast to virus release, also requires lipid rafts.

Since the cell-cell fusion processes are mediated mainly by the viral S protein, we examined whether S proteins are involved in lipid rafts during cell-cell fusion. As shown above (Fig. 6B), a small fraction of S protein on the plasma membrane was associated with detergent-resistant membrane fractions, consistent with the interpretation that the S protein-mediated cell-cell fusion involves lipid rafts. Furthermore, we found that some of the S protein, when overexpressed alone in 293A cells, localized in detergent-resistant fractions (Fig. 8A), indicating that S protein does not require other viral proteins for association with lipid rafts.

Finally, we tried to identify the domains in the S protein required for the association with lipid rafts. Three truncated mutants of S protein were generated by manipulating the nature of the transmembrane domain and length of the cytoplasmic tails (Fig. 8B, left): S-C9, which contained only nine amino acids in the cytoplasmic tail; S-C0, which did not have any cytoplasmic tails; and S-CV, where the transmembrane domain was replaced by the transmembrane domain of vesicular stomatitis virus glycoprotein G. It has been reported that vesicular stomatitis virus glycoprotein G does not associate with lipid rafts (30, 39). All the three truncated mutants of S protein were expressed in similar amounts in the cells (Fig. 8B, left, bottom). S-C9 and S-C0 proteins were associated with lipid rafts, whereas S-CV was not (Fig. 8B, right). Thus, the transmembrane domain of S protein is important for its interaction with lipid rafts.

DISCUSSION

Thorp and Gallagher (37) first reported that MHV entry and cell-cell fusion were greatly affected by the depletion of cholesterol. This result was puzzling, since MHVR was shown to

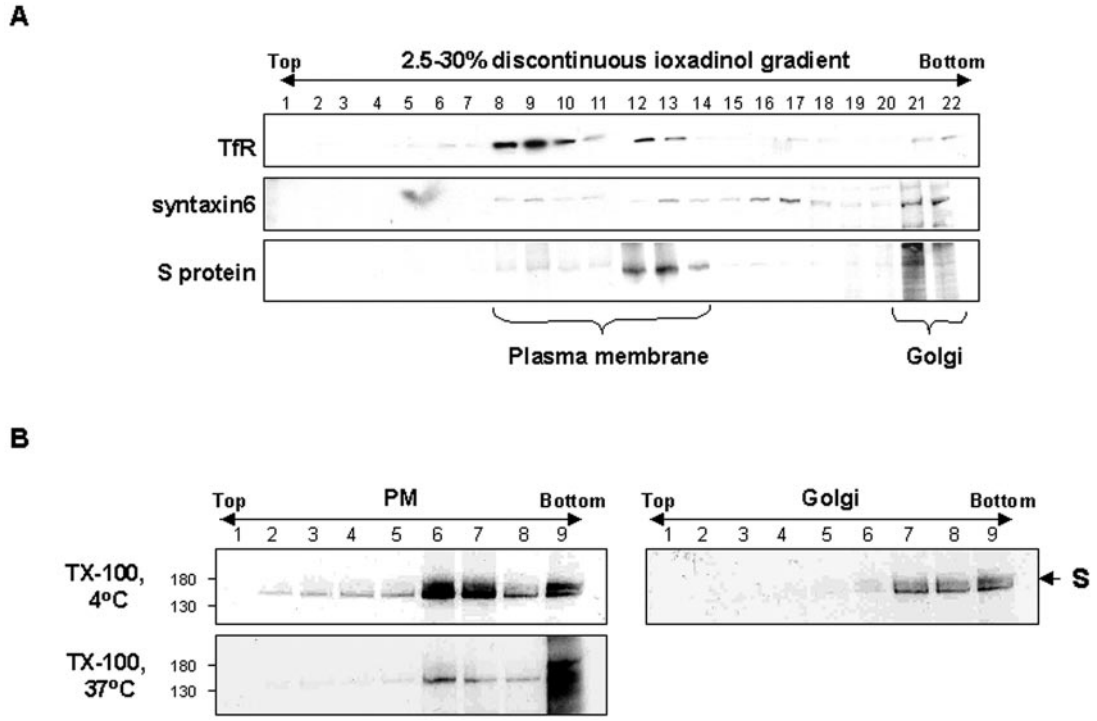

FIG. 6. Raft-association of the viral S proteins in plasma and Golgi membranes. (A) Fractionation of total membranes into plasma and Golgi membranes. Membranes prepared from ^{35}S-translabeled MHV-infected cells were fractionated in a 2.5%, 10%, 17.5%, and 25% iodixanol step gradient. Samples were collected into 0.8-ml fractions. Transferrin receptor (TfR) and syntaxin 6 were used as plasma and Golgi membrane markers, respectively. S proteins were detected by immunoprecipitation with polyclonal anti-MHV antibody. (B) Association of viral proteins from plasma and Golgi membranes with lipid rafts. Fractions from lanes 8 to 14 or 21 and 22 of panel A were pooled and analyzed by membrane flotation gradients. Viral proteins were detected by immunoprecipitation with polyclonal anti-MHV antibody.

be not associated with lipid rafts. These findings were confirmed in the current study. We further showed that MHV did not incorporate lipid rafts into virion. The additional experiments presented in our studies reported here provided explanations for these confounding observations. We found that MHV bound initially to the nonraft membrane (at 4°C), presumably through MHVR. As virus entry occurred (at 37°C), the viral spike protein became associated with lipid rafts (Fig. 4A). When cholesterol was depleted, viral entry could not occur even though the virus still bound to the membrane (Fig. 3A and 4B). Thus, there is a redistribution of MHV from nonraft membrane to lipid rafts during virus entry, and the association of viral S protein with lipid rafts is critical for virus entry. This redistribution very likely involves cellular factors that interact with either MHVR or viral S protein after virus binds to MHVR. This membrane shift has also been observed for another coronavirus, HCoV-229E (23). The internalization of HCoV-229E was decreased by the depletion of cholesterol, while the binding of virus was not affected. Therefore, the redistribution of the bound virus to lipid rafts before virus internalization can take place may be a common process in coronavirus. In the case of HCoV-229E, the redistribution process involves the sequestration of the viral receptor, CD13, to caveolae (23). At this time, it has not been demonstrated whether caveolae are also involved in MHV entry. It is possible that some host factors that interact with S protein may be relocalized to caveolae during MHV entry. However, this factor cannot be MHVR, since MHVR did not relocalize to lipid rafts during virus infection. Moreover, it has been shown that forced association of MHVR with lipid rafts by addition of the glycosylphosphatidyl inositol anchor did not enhance virus infectivity (37), indicating that the association of MHVR with lipid rafts does not happen and is not required for virus entry. Similar observation was made for herpes simplex virus (4); its cellular receptors, herpesvirus entry mediator and nectin-1, did not associate with lipid rafts, but one of the viral glycoproteins (gD) was found associated with lipid rafts, suggesting that unknown cellular cofactors mediate the recruitment of gD to lipid rafts.

We also found that MHV assembly and release did not involve lipid rafts. Consistent with this observation, we found that the viral S protein on the Golgi membrane, where MHV virion is assembled and released, is not associated with lipid rafts, even though the Golgi membrane is known to contain lipid rafts (33). This finding is in contrast to many other enveloped viruses, such as HIV, which contain lipid rafts in the virion and in which the viral proteins involved in the assembly and budding of virions are associated with lipid rafts (13). Significantly, the MHV S protein is associated with lipid rafts in the plasma membrane; correspondingly, the cell-cell fusion induced by MHV is affected by cholesterol depletion. The possible explanation for the differential properties of S protein in the plasma and Golgi membranes is that S proteins may be recruited to lipid rafts through the interaction with an unidentified factor that is present in the plasma membrane but is missing in the Golgi. This factor is

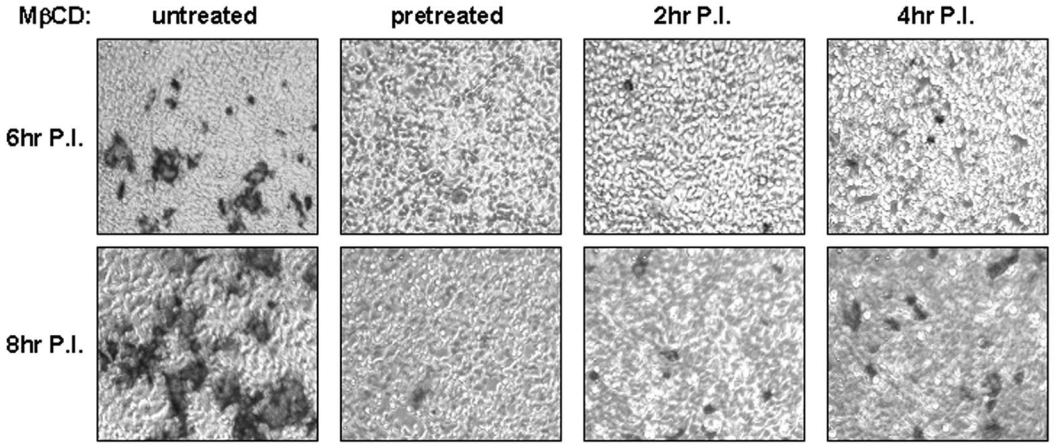

FIG. 7. Inhibition of cell-cell fusion by MβCD. Cells were treated with 10 mM MβCD for 30 min at several different time points during virus infection: pretreatment and after being treated at 2 and 4 h p.i. Cells were fixed at 6 and 8 h p.i. and immunostained with anti-N monoclonal antibody, followed by incubation with β-galactosidase-conjugated secondary antibody. Syncytium formation was visualized by X-Gal (5-bromo-4-chloro-3-indolyl-β-galactoside) staining (shown as dark areas).

likely neither MHVR nor other viral proteins, since MHVR did not associate with lipid rafts, and S protein alone could associate with lipid rafts.

The observations that both virus entry and cell-cell fusion were inhibited by cholesterol depletion imply that lipid rafts may be involved in both processes following a common mechanism. Both processes are initiated by the binding of S protein to MHVR, followed by fusion between two different membranes (virus-cell or cell-cell). In the case of virus entry, the S-MHVR binding triggers the relocalization of the virus to a lipid raft membrane. In the case of cell-cell fusion, S protein is localized on lipid rafts on the plasma membrane. Thus, the association of S protein with lipid rafts is likely crucial for virus entry and cell-cell fusion.

A number of studies have shown that enveloped viruses, such as HIV, contain lipid rafts in the virion, and viral proteins

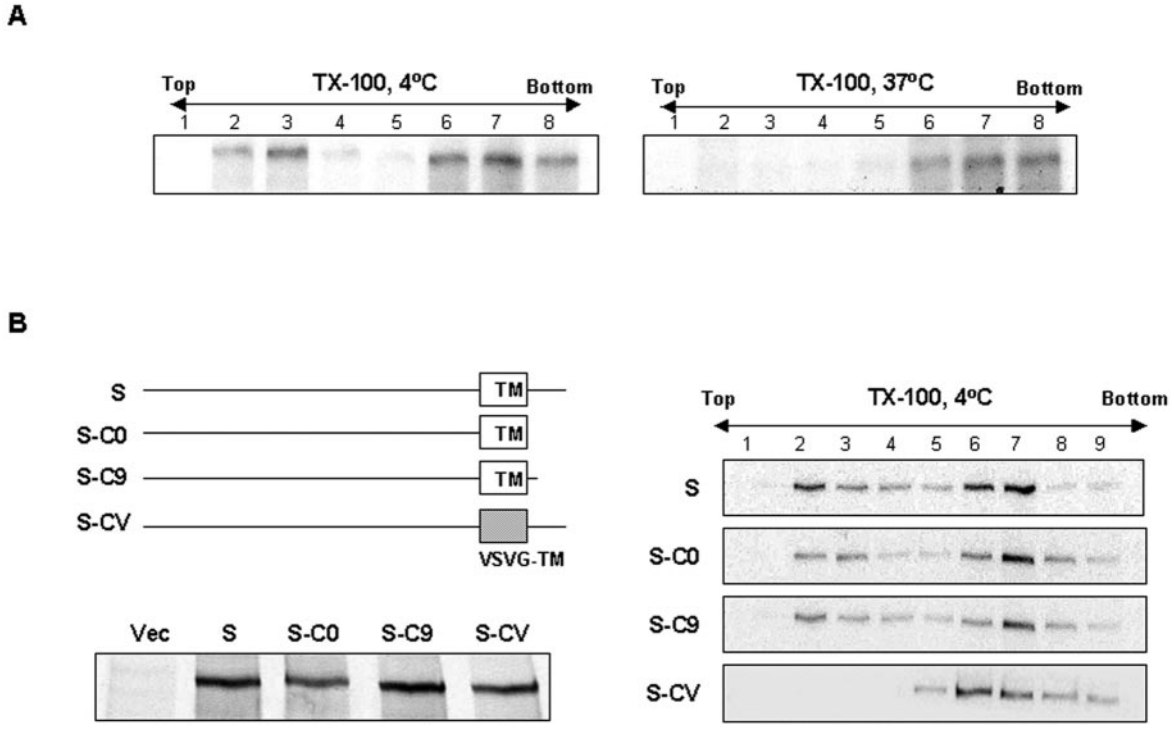

FIG. 8. Determination of raft association domains of S proteins. (A) Raft association of S protein overexpressed in 293A cells. (B) Domains required for lipid raft association of S protein. (Left, top) Diagram of S protein mutants. (Bottom) The expression level of mutants was determined by immunoprecipitation with anti-MHV polyclonal antibody from ^{35}S-translabeled cellular lysates. Membrane flotation analysis was done for the truncated mutants (right).

that are required for virus assembly and budding associate with lipid rafts (13, 17). While most of the studies so far have focused on the viruses that bud out of the plasma membrane, the viruses that bud out of the intracellular membranes have not been carefully examined. Cholesterol, which is a major component of lipid rafts, is abundant in the plasma membranes and endosome, but due to the recycling of cholesterol transport, it is also present in the Golgi membrane (33). Therefore, it could not be ruled out completely that MHV, which assembles and buds on the Golgi membrane, may somehow involve lipid rafts during its maturation process.

In conclusion, MHV requires lipid rafts in virus entry and cell-cell fusion but not in virus release. The involvement of lipid rafts is mediated by the direct or indirect interaction of S protein with lipid rafts.

ACKNOWLEDGMENT

This work was partially supported by National Institutes of Health research grant AI19244.

REFERENCES

1. **Ahn, A., D. L. Gibbons, and M. Kielian.** 2002. The fusion peptide of Semliki Forest virus associates with sterol-rich membrane domains. J. Virol. **76:** 3267–3275.
2. **Ali, A., R. T. Avalos, E. Ponimaskin, and D. P. Nayak.** 2000. Influenza virus assembly: effect of influenza virus glycoproteins on the membrane association of M1 protein. J. Virol. **74:**8709–8719.
3. **Bavari, S., C. M. Bosio, E. Wiegand, G. Ruthel, A. B. Will, T. W. Geisbert, M. Hevey, C. Schmaljohn, A. Schmaljohn, and M. J. Aman.** 2002. Lipid raft microdomains: a gateway for compartmentalized trafficking of Ebola and Marburg viruses. J. Exp. Med. **195:**593–602.
4. **Bender, F. C., J. C. Whitbeck, M. Ponce de Leon, H. Lou, R. J. Eisenberg, and G. H. Cohen.** 2003. Specific association of glycoprotein B with lipid rafts during herpes simplex virus entry. J. Virol. **77:**9542–9552.
5. **Bock, J. B., J. Klumperman, S. Davanger, and R. H. Scheller.** 1997. Syntaxin 6 functions in *trans*-Golgi network vesicle trafficking. Mol. Biol. Cell **8:**1261–1271.
6. **Braunwald, J., H. Nonnenmacher, C. A. Pereira, and A. Kirn.** 1991. Increased susceptibility to mouse hepatitis virus type 3 (MHV3) infection induced by a hypercholesterolaemic diet with increased adsorption of MHV3 to primary hepatocyte cultures. Res. Virol. **142:**5–15.
7. **Brown, D. A., and E. London.** 1998. Structure and origin of ordered lipid domains in biological membranes. J. Membr. Biol. **164:**103–114.
8. **Campbell, S. M., S. M. Crowe, and J. Mak.** 2002. Virion-associated cholesterol is critical for the maintenance of HIV-1 structure and infectivity. AIDS **16:**2253–2261.
9. **Cerny, J., H. Stockinger, and V. Horejsi.** 1996. Noncovalent associations of T lymphocyte surface proteins. Eur. J. Immunol. **26:**2335–2343.
10. **Chazal, N., and D. Gerlier.** 2003. Virus entry, assembly, budding, and membrane rafts. Microbiol. Mol. Biol. Rev. **67:**226–237.
11. **Daya, M., M. Cervin, and R. Anderson.** 1988. Cholesterol enhances mouse hepatitis virus-mediated cell fusion. Virology **163:**276–283.
12. **Del G. Real, S. Jimenez-Baranda, R. A. Lacalle, E. Mira, P. Lucas, C. Gomez-Mouton, A. C. Carrera, A. C. Martinez, and S. Manes.** 2002. Blocking of HIV-1 infection by targeting CD4 to nonraft membrane domains. J. Exp. Med. **196:**293–301.
13. **Graham, D. R., E. Chertova, J. M. Hilburn, L. O. Arthur, and J. E. Hildreth** 2003. Cholesterol depletion of human immunodeficiency virus type 1 and simian immunodeficiency virus with β-cyclodextrin inactivates and permeabilizes the virions: evidence for virion-associated lipid rafts. J. Virol. **77:** 8237–8248.
14. **Harder, T., P. Scheiffele, P. Verkade, and K. Simons.** 1998. Lipid domain structure of the plasma membrane revealed by patching of membrane components. J. Cell Biol. **141:**929–942.
15. **Harris, T. J., and C. H. Siu.** 2002. Reciprocal raft-receptor interactions and the assembly of adhesion complexes. Bioessays **24:**996–1003.
16. **Hirano, N., K. Fujiwara, S. Hino, and M. Matumoto.** 1974. Replication and plaque formation of mouse hepatitis virus (MHV-2) in mouse cell line DBT culture. Arch. Gesamte Virusforsch. **44:**298–302.
17. **Holm, K., K. Weclewicz, R. Hewson, and M. Suomalainen.** 2003. Human immunodeficiency virus type 1 assembly and lipid rafts: $Pr55^{gag}$ associates with membrane domains that are largely resistant to Brij98 but sensitive to Triton X-100. J. Virol. **77:**4805–4817.
18. **Klumperman, J., J. K. Locker, A. Meijer, M. C. Horzinek, H. J. Geuze, and P. J. Rottier.** 1994. Coronavirus M proteins accumulate in the Golgi complex beyond the site of virion budding. J. Virol. **68:**6523–6534.
19. **Kovbasnjuk, O., M. Edidin, and M. Donowitz.** 2001. Role of lipid rafts in Shiga toxin 1 interaction with the apical surface of Caco-2 cells. J. Cell Sci. **114:**4025–4031.
20. **Kozak, S. L., J. M. Heard, and D. Kabat.** 2002. Segregation of CD4 and CXCR4 into distinct lipid microdomains in T lymphocytes suggests a mechanism for membrane destabilization by human immunodeficiency virus. J. Virol. **76:**1802–1815.
21. **Lee, A.** 2001. Membrane structure. Curr. Biol. **11:**R811–R814.
22. **Marjomaki, V., V. Pietiainen, H. Matilainen, P. Upla, J. Ivaska, L. Nissinen, H. Reunanen, P. Huttunen, T. Hyypia, and J. Heino.** 2002. Internalization of echovirus 1 in caveolae. J. Virol. **76:**1856–1865.
23. **Nomura, R., A. Kiyota, E. Suzaki, K. Kataoka, Y. Ohe, K. Miyamoto, T. Senda, and T. Fujimoto.** 2004. Human coronavirus 229E binds to CD13 in rafts and enters the cell through caveolae. J. Virol. **78:**8701–8708.
24. **Ono, A., and E. O. Freed.** 2001. Plasma membrane rafts play a critical role in HIV-1 assembly and release. Proc. Natl. Acad. Sci. USA **98:**13925–13930.
25. **Panchal, R. G., G. Ruthel, T. A. Kenny, G. H. Kallstrom, D. Lane, S. S. Badie, Li, L., S. Bavari, and M. J. Aman.** 2003. In vivo oligomerization and raft localization of Ebola virus protein VP40 during vesicular budding. Proc. Natl. Acad. Sci. USA **100:**15936–15941.
26. **Parton, R. G., and M. Lindsay.** 1999. Exploitation of major histocompatibility complex class I molecules and caveolae by simian virus 40. Immunol. Rev. **168:**23–31.
27. **Pickl, W. F., F. X. Pimentel-Muinos, and B. Seed.** 2001. Lipid rafts and pseudotyping. J. Virol. **75:**7175–7183.
28. **Popik, W., T. M. Alce, and W. C. Au.** 2002. Human immunodeficiency virus type 1 uses lipid raft-colocalized CD4 and chemokine receptors for productive entry into $CD4^+$ T cells. J. Virol. **76:**4709–4722.
29. **Rawat, S. S., M. Viard, S. A. Gallo, A. Rein, R. Blumenthal, and A. Puri.** 2003. Modulation of entry of enveloped viruses by cholesterol and sphingolipids (Review). Mol. Membr. Biol. **20:**243–254.
30. **Scheiffele, P., A. Rietveld, T. Wilk, and K. Simons.** 1999. Influenza viruses select ordered lipid domains during budding from the plasma membrane. J. Biol. Chem. **274:**2038–2044.
31. **Scheiffele, P., M. G. Roth, and K. Simons.** 1997. Interaction of influenza virus haemagglutinin with sphingolipid-cholesterol membrane domains via its transmembrane domain. EMBO J. **16:**5501–5508.
32. **Simons, K., and E. Ikonen.** 1997. Functional rafts in cell membranes. Nature **387:**569–572.
33. **Simons, K., and E. Ikonen.** 2000. How cells handle cholesterol. Science **290:**1721–1726.
34. **Simons, K., and D. Toomre.** 2000. Lipid rafts and signal transduction. Nat. Rev. Mol. Cell Biol. **1:**31–39.
35. **Singer, S. J., and G. L. Nicolson.** 1972. The fluid mosaic model of the structure of cell membranes. Science **175:**720–731.
36. **Suomalainen, M.** 2002. Lipid rafts and assembly of enveloped viruses. Traffic **3:**705–709.
37. **Thorp, E. B., and T. M. Gallagher.** 2004. Requirements for CEACAMs and cholesterol during murine coronavirus cell entry. J. Virol. **78:**2682–2692.
38. **Tsui-Pierchala, B. A., M. Encinas, J. Milbrandt, and E. M. Johnson, Jr.** 2002. Lipid rafts in neuronal signaling and function. Trends Neurosci. **25:** 412–417.
39. **Vincent, S., D. Gerlier, and S. N. Manie.** 2000. Measles virus assembly within membrane rafts. J. Virol. **74:**9911–9915.
40. **Yokomori, K., and M. M. C. Lai.** 1992. The receptor for mouse hepatitis virus in the resistant mouse strain SJL is functional: implications for the requirement of a second factor for viral infection. J. Virol. **66:**6931–6938.